Review

Cancer Research

A Comprehensive Survey of Ras Mutations in Cancer

Ian A. Prior[1], Paul D. Lewis[2], and Carla Mattos[3]

Abstract

All mammalian cells express 3 closely related Ras proteins, termed H-Ras, K-Ras, and N-Ras, that promote oncogenesis when they are mutationally activated at codon 12, 13, or 61. Although there is a high degree of similarity among the isoforms, K-Ras mutations are far more frequently observed in cancer, and each isoform displays preferential coupling to particular cancer types. We examined the mutational spectra of Ras isoforms curated from large-scale tumor profiling and found that each isoform exhibits surprisingly distinctive codon mutation and amino-acid substitution biases. These findings were unexpected given that these mutations occur in regions that share 100% amino-acid sequence identity among the 3 isoforms. Of importance, many of these mutational biases were not due to differences in exposure to mutagens, because the patterns were still evident when compared within specific cancer types. We discuss potential genetic and epigenetic mechanisms, as well as isoform-specific differences in protein structure and signaling, that may promote these distinct mutation patterns and differential coupling to specific cancers. *Cancer Res; 72(10); 2457–67. ©2012 AACR.*

Introduction

Ras proteins are proto-oncogenes that are frequently mutated in human cancers. They are encoded by 3 ubiquitously expressed genes: HRAS, KRAS, and NRAS. These proteins are GTPases that function as molecular switches in regulating pathways that are responsible for proliferation and cell survival. Normally, Ras proteins are tightly regulated by guanine nucleotide exchange factors (GEF) that promote GDP dissociation and GTP binding, and GTPase-activating proteins (GAP) that stimulate the intrinsic GTPase activity of Ras to switch off signaling. Aberrant Ras function is associated with hyperproliferative developmental disorders and cancer, and in tumors is associated with a single mutation typically at codon 12, 13, or 61 (1). Mutation at these conserved sites favors GTP binding and produces constitutive activation of Ras (Fig. 1). Of importance, all Ras isoforms share sequence identity in all of the regions that are responsible for GDP/GTP binding, GTPase activity, and effector interactions, suggesting a functional redundancy. Nevertheless, it is becoming increasingly apparent that Ras proteins have isoform-specific functions (2). These functional differences are most likely associated with the unique C-terminal hypervariable region (HVR) in each isoform, which is thought to modulate the Ras–membrane interaction to specify distinctive localizations in organelles and signaling nanoclusters (3).

Authors' Affiliations: [1]Physiological Laboratory, Department of Molecular and Cellular Physiology, Institute of Translational Research, University of Liverpool, Liverpool; [2]Cancer Informatics Group, Institute of Life Science, Swansea University, Swansea, United Kingdom; [3]Department of Chemistry and Chemical Biology, Northeastern University, Boston, Massachusetts

Corresponding Author: Ian A. Prior, Physiological Laboratory, University of Liverpool, Crown Street, Liverpool L69 3BX, UK. Phone: 44-151-794-5332; Fax: 44-151-794-4434; E-mail: iprior@liv.ac.uk

doi: 10.1158/0008-5472.CAN-11-2612

An intriguing observation from the early days of Ras research is that different types of cancer appear to be coupled to mutation of a particular Ras isoform (4). We revisited this unexplained phenomenon by using the latest data from a large-scale collation of tumor sequencing to reveal additional patterns of isoform-specific codon and point mutation biases. We discuss the effects of these mutations on Ras function, and potential mechanisms that may lead to differential patterns of Ras isoform mutations.

Ras Mutation Frequencies

Large-scale tumor profiling

Early analyses of Ras isoform mutational status in cancer revealed varying incidences of Ras mutations in different tumor types, and specific associations of individual Ras isoforms with particular cancers (4). Despite the relatively small sample sizes used in those analyses, investigators were able to identify strong trends. For example, K-Ras was shown to be the most frequently mutated isoform in most cancers, with 90% of pancreatic tumors harboring K-Ras mutations. In contrast, N-Ras mutations were more strongly associated with hematopoietic tumors. With the advent of large-scale tumor profiling and data sequencing databases, researchers can now perform deeper analyses of Ras mutational spectra. The Catalog of Somatic Mutations in Cancer (COSMIC) is the most comprehensive database on human tumor mutations currently available (5).

The COSMIC dataset confirms that K-Ras is the most frequently mutated isoform. It was found to be present in 22% of all tumors analyzed, compared with 8% for N-Ras and 3% for H-Ras (Table 1). These headline values would seem to support the often-cited compound mutation rate of 30%; however, this value is distorted by the screening bias that is evident within the dataset, particularly for K-Ras, where colorectal cancer dominates the data totals. When all cancers in which at least 20 tumors were counted are given equal weighting, the average pan-Ras mutation incidence is 16%.

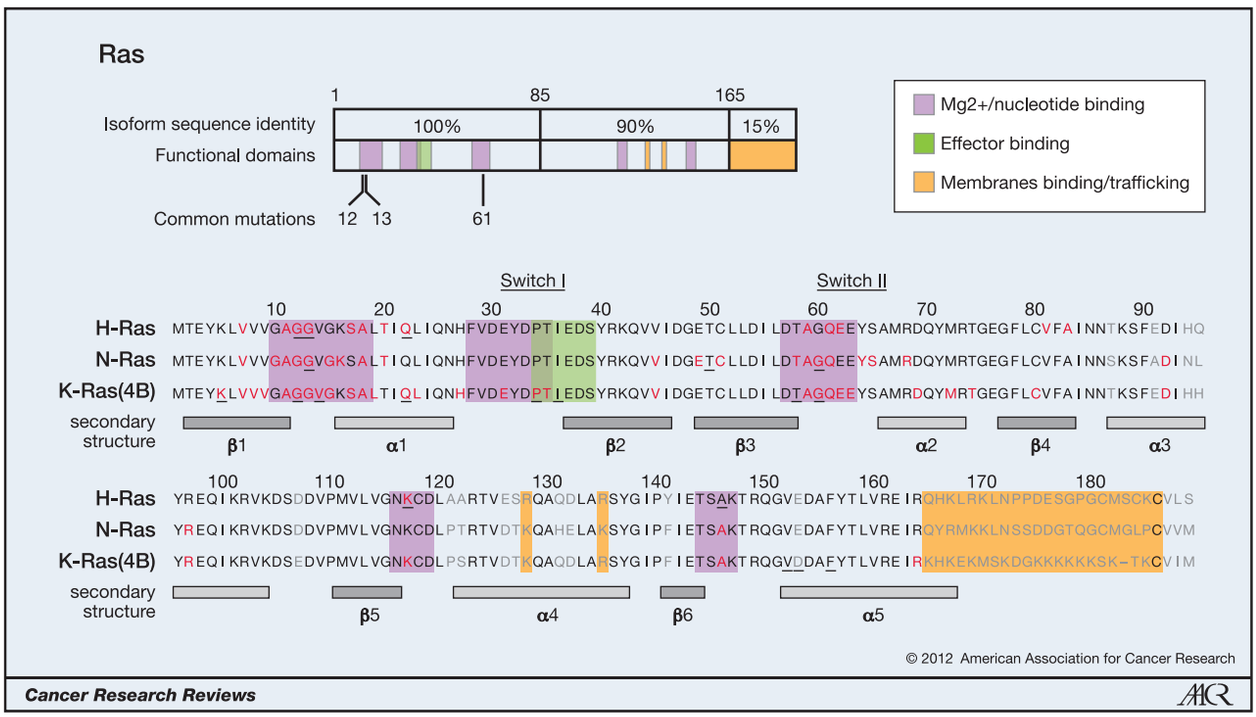

Figure 1. Oncogenic mutations of Ras isoforms. The key oncogenic mutations are in the region that is identical among the 3 isoforms. Forty-four separate point mutations have been characterized in Ras isoforms, with 99.2% of all mutations occurring at codons 12, 13, and 61. Mutations that cluster in and around loops 1, 2, and 4 are responsible for nucleotide binding and result in enhanced GTP binding. Residues that are mutated in cancer are highlighted in red, those that are mutated in developmental disorders are underlined, and those that are variable among isoforms are in gray (26, 65, 66).

With the exception of the salivary gland, screening has focused on the locations and isoforms with the strongest coupling. Of note, however, the mutation rate in the pancreas is 60% rather than the generally quoted 90%. In most cases, 1 isoform dominates the number of mutations scored for a particular cancer. One exception is thyroid cancer, in which large numbers of mutants of all 3 isoforms have been counted. Although these observations confirm known trends, a comparison of codon mutations among the Ras isoforms reveals some intriguing deeper patterns.

Codon specificity of Ras isoform mutations

In analogy to the isoform bias we can see in specific cancers, analyses of codon mutation frequencies reveal that each isoform has a distinctive codon mutation signature (Fig. 2). K-Ras and N-Ras represent 2 extremes of this phenomenon: 80% of K-Ras mutations occur at codon 12, whereas very few mutations are observed at codon 61. In contrast, almost 60% of N-Ras tumors harbor mutations at codon 61, compared with 35% at codon 12. H-Ras displays an intermediate behavior, with an approximately 50%/40% split between mutations at codons 12 and 61, respectively. These data represent averages of the percentages for each cancer in which at least 20 tumors were scored. Of importance, a closer examination of trends within different cancers confirms the individuality of each isoform even in circumstances in which the isoforms presumably have been exposed to common mutagenic factors (Fig. 2B).

These differences in codon specificity are surprising because all 3 oncogenic mutations are in amino-acid regions that are identical among the 3 isoforms and are assumed to generate equivalent effects on protein activity. Of note, even at the DNA level, K-Ras and N-Ras share identical sequences encoding Gly12 and Gln61. Furthermore, individual single-base substitutions result in the same amino-acid replacement for all of the isoforms. Nevertheless, an examination of the preferred single-base substitutions collated from all Ras-mutated tumors in the COSMIC database reveals a final level of difference among the isoforms (Table 2).

Ras codons 12, 13, and 61 can each be converted to 6 other amino acids via single-base substitutions. However, >60% of the total mutations for each isoform are accounted for by only 3 of the 18 potential mutations across the codons (Table 2). K-Ras mutation patterns are dominated by the 43% of mutations that are G→A transitions at the second base of codons 12 or 13, resulting in G12D or G13D mutations. G→T transversions at the second base make up the bulk of the remainder to produce G12V. A special case is observed in lung cancer, where a G→T transversion of the first base of codon 12 to produce G12C predominates. N-Ras favors similar types of mutations at codons 12 and 13, albeit at much lower rates compared with K-Ras. In contrast, H-Ras favors G12V in all cancers with codon 12 mutations, and more generally exhibits a 3-fold higher proportion of transversion-to-transition mutations compared with K-Ras and N-Ras. Mutations at codon 61 recapitulate the heterogeneity that is evident between isoforms at codon 12.

These data reveal that Ras isoforms exhibit differential and preferential coupling to specific cancers, codons, and base substitutions. The distinct mutation patterns exhibited by Ras

Table 1. Incidence of Ras isoform mutations in cancer

	HRAS			KRAS			NRAS			Pan-Ras
Primary tissue	+	***n***	**%**	+	***n***	**%**	+	***n***	**%**	**%**
Adrenal gland	1	135	<1%	1	210	<1%	7	170	4%	5%
Autonomic ganglia	0	63	0%	2	63	3%	7	102	7%	10%
Biliary tract	0	151	0%	460	1,471	31%	3	213	1%	33%
Bone	3	147	2%	2	165	1%	0	143	0%	3%
Breast	5	542	<1%	20	544	4%	7	330	2%	7%
Central nervous system	0	942	0%	8	1,032	<1%	8	995	<1%	2%
Cervix	23	264	9%	46	637	7%	2	132	2%	17%
Endometrium	3	291	1%	298	2,108	14%	1	279	<1%	16%
Hematopoietic/lymphoid	8	3,074	<1%	277	5,757	5%	877	8,540	10%	15%
Kidney	1	273	<1%	4	617	<1%	2	435	<1%	1%
Large intestine	2	617	<1%	9,671	29,183	33%	26	1,056	3%	36%
Liver	0	270	0%	21	450	5%	8	310	3%	7%
Lung	9	1,957	<1%	2,533	14,632	17%	26	2,678	1%	19%
Esophagus	2	161	1%	13	359	4%	0	161	0%	5%
Ovary	0	94	0%	406	2,934	14%	5	111	5%	18%
Pancreas	0	221	0%	3,127	5,169	61%	5	248	2%	63%
Prostate	29	500	6%	82	1,024	8%	8	530	2%	15%
Salivary gland	24	161	15%	5	170	3%	0	45	0%	18%
Skin	120	1,940	6%	38	1,405	3%	858	4,742	18%	27%
Small intestine	0	5	0%	62	316	20%	0	5	0%	20%
Stomach	14	384	4%	163	2,571	6%	5	215	2%	12%
Testis	5	130	4%	17	432	4%	8	283	3%	11%
Thymus	1	46	2%	4	186	2%	0	46	0%	4%
Thyroid	117	3,601	3%	137	4,628	3%	312	4,126	8%	14%
Upper aerodigestive tract	101	1,083	9%	52	1,535	3%	24	807	3%	16%
Urinary tract	138	1,242	11%	29	591	5%	9	398	2%	18%
Total	606	18,294	3%	17,478	78,189	22%	2,208	27,100	8%	16%

Most cancer types favor mutation of a single isoform (typically K-Ras). Data are collated from COSMIC v52 release. +, the number of tumors observed with the mutant Ras; *n*, the number of unique samples screened.

isoforms raise fundamental questions about their etiology. For example, do the mutation patterns reflect genetic or epigenetic differences between Ras isoforms that may lead to differential targeting of mutagens or repair processes? Additionally, how is this influenced by protein-level effects such as relative Ras isoform abundance in tissues, cells, and subcellular compartments, or possibly isoform-specific differences in the effects of individual mutations on activity that combine to modulate the signaling output and hence the relative oncogenicity?

Ras mutation etiology

Many genotoxic agents have been implicated in causing Ras mutations. Investigators have identified sequence motifs that correlate with highly reproducible mutagenesis. For example, classic chemical carcinogenesis studies showed that methylnitrosourea targets the second base of codon 12 of H-Ras and K-Ras in a variety of cancer types to generate G12D mutations (6, 7). In contrast, UV radiation targets pyrimidine dimers, resulting in a high bias toward generating Ras Q61 mutations (8). The general trends in the dataset indicate predominantly bulky-adduct–induced damage for K-Ras mutations at codon 12, and chemical- or UV-radiation–induced damage for Q61 mutations in N-Ras.

It is clear that some of the observed mutational heterogeneity is due to tissue-specific exposure to different cocktails of mutagens. This is particularly the case when mutation patterns are compared across a single isoform. For example, lung cancer shows a highly distinctive coupling to G12C mutations (Table 2). The G.C→T.A transversions that generate the G12C mutation were associated in *in vitro* studies with the formation of bulky DNA adducts by tobacco-smoke products (9). This specific mutation is most common in current smokers, and its incidence progressively declines to zero in former and never smokers (10). Although G12C appears to be a diagnostic mutation of exposure to tobacco-smoke mutagens, it is far less abundant in pancreatic and colorectal cancers that are also strongly linked to smoking, indicating tissue-specific differences in exposure to individual tobacco mutagens (11–13).

Other examples of potential tissue-specific mutagen exposure are colorectal cancer and hematopoietic/lymphoid cancers, where K-Ras and N-Ras exhibit unusually high

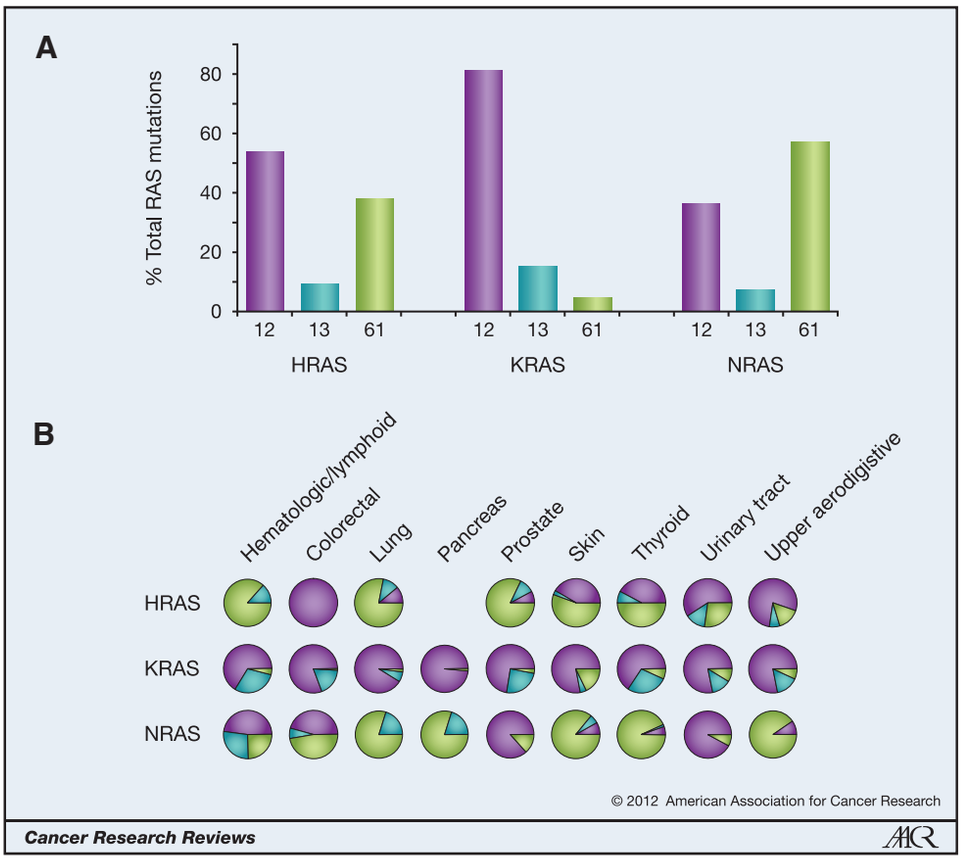

Figure 2. Ras-isoform–specific codon mutation bias. A, K-Ras is typically mutated at codon 12, whereas N-Ras favors codon 61. H-Ras displays intermediate behavior. Data are averages of percentages collated from all cancers with at least 20 tumors scored. B, analysis of individual cancer types reveals isoform-specific patterns of codon mutation even within the same tissue. Pie chart colors: black, codon 12; gray, codon 13; white, codon 61.

preponderances of codon 13 mutations. Of interest, in advanced colorectal cancer, G13D mutations have prognostic significance in anti–epidermal growth factor receptor (anti-EGFR) cetuximab-based therapy (14). This drug is not given to patients with K-Ras mutations, because those with G12 mutations do not respond. However, patients with G13-mutated tumors showed significant improvements in survival, indicating the importance of discriminating between Ras codon mutation types when designing clinical trials and treatment programs.

Genetic and epigenetic influences

Some of this mutational bias implies differential exposure to mutagens. Although this may account for the distinct mutations of K-Ras found in different cancers, it does not explain why there is a difference between isoforms within the same cancer. The best example of this is thyroid carcinoma, in which significant numbers of mutations of all isoforms have been identified. In particular, this type of cancer has been linked to exposure to ionizing radiation as well as to various chemical carcinogens (15). A comparison of mutation patterns across the Ras isoforms reveals a clear bias, with 95% of N-Ras mutations occurring at codon 61 and 66% of K-Ras mutations occurring at codon 12. In analogy to the headline trends seen across all cancers, H-Ras has an intermediate profile, with a 40%/50% split between codon 12 and codon 61, respectively. Within the codons, the mutation patterns are also distinctive. For example, at codon 12, K-Ras is predominantly G12D mutated, whereas H-Ras favors G12V.

To date, few experimental analyses have focused on potential reasons for these differences. However, we can use the available empirical data and draw some inferences from a larger number of studies carried out using the TP53 gene. We can then speculate that the heterogeneity may be due to variables such as the DNA primary sequence, secondary-quaternary structural effects, and the position of the Ras genes within the genome and the nucleus. Together, these effects may improve or limit the access of different mutagens or repair enzymes.

Of importance, Ras-isoform–specific differences in rates of DNA damage and repair have been identified. Feng and colleagues (16) measured both adduct formation and subsequent repair of Ras isoforms following exposure to various bulky carcinogens, including benzo[a]pyrene diol epoxide (BPDE). They showed that although codon 12 was the preferred binding site for BPDE on K-Ras, adduct levels were reduced at this site in N-Ras and H-Ras. Other carcinogens that have different

Table 2. Isoform-specific point mutation specificity

HRAS		Codon 12: GGC						Codon 13: GGT						Codon 61: CAG						
		-C-	T–	-A-	C–	A–	-T-	-C-	T–	-A-	C–	A–	-T-	G–	–C/T	A–	-T-	-C-	-G-	
Primary tissue	Cancer	12A	12C	12D	12R	12S	12V	13A	13C	13D	13R	13S	13V	61E	61H	61K	61L	61P	61R	Total
Prostate	Adenocarcinoma	0	0	0	0	1	1	0	0	0	3	0	0	0	3	0	18	0	3	29
Salivary gland	Adenocarcinoma	0	0	1	4	1	8	0	0	0	3	0	0	0	0	0	0	0	6	23
Skin	Benign melanocytic nevus	0	0	0	1	0	0	0	0	0	1	0	0	0	1	1	20	0	11	35
	Carcinoma	0	2	2	0	0	24	0	0	1	0	0	0	0	3	0	3	0	0	35
	Malignant melanoma	0	0	0	0	0	2	0	0	1	0	0	0	0	1	2	3	0	2	11
Stomach	Adenocarcinoma	0	0	0	0	0	14	0	0	0	0	0	0	0	0	0	0	0	0	14
Thyroid	Adenoma-nodule-goiter	0	0	0	0	0	19	0	0	0	0	0	0	0	1	4	0	1	16	41
	Carcinoma	2	2	2	1	2	19	0	2	3	6	0	0	0	2	10	1	1	23	76
Urinary tract	Bladder carcinoma	0	4	9	0	6	90	0	3	0	2	0	3	0	0	6	6	0	9	138
Upper aerodigestive	Mouth	0	5	3	2	24	14	0	1	3	4	1	4	0	3	0	3	0	9	76
	Total	2	13	17	8	34	191	0	6	8	19	1	7	0	14	23	54	2	79	478

KRAS		Codon 12: GGT						Codon 13: GGC						Codon 61: CAA						
		-C-	T–	-A-	-C–	A–	-T-	-C-	T–	-A-	C–	A–	-T-	G–	–C/T	A–	-T-	-C-	-G-	
Primary tissue	Cancer	12A	12C	12D	12R	12S	12V	13A	13C	13D	13R	13S	13V	61E	61H	61K	61L	61P	61R	Total
Biliary tract	Bile duct carcinoma	14	29	107	6	30	49	0	5	12	0	1	0	0	2	0	0	0	0	255
Gall bladder	Carcinoma	0	5	60	9	12	10	0	0	1	1	0	0	0	0	0	0	0	0	98
Colorectal	Colon adenocarcinoma	107	184	635	18	133	364	0	10	338	6	3	3	0	5	1	4	0	1	1,812
	Rectal adenocarcinoma	37	45	178	4	33	124	0	6	88	4	0	3	0	5	0	3	0	2	532
Endometrium	Carcinoma	39	26	121	3	12	68	2	4	26	0	1	1	0	3	0	0	0	0	306
H/L	Hematopoietic neoplasm	8	4	38	2	10	12	0	0	25	0	0	0	0	4	1	2	0	0	106
	Lymphoid neoplasm	19	7	43	4	10	10	0	0	48	0	1	0	0	3	0	0	3	0	148
Lung	Adenocarcinoma	106	545	222	27	59	279	1	43	31	1	1	1	0	11	1	5	0	2	1,335
	Bronchioloalveolar adenocarcinoma	6	42	38	3	4	33	0	2	0	0	0	0	0	0	0	0	0	0	128
	Non–small cell carcinoma	34	283	113	14	30	112	0	23	20	1	1	1	1	6	4	1	1	5	650
	Squamous cell carcinoma	3	25	26	5	6	10	0	0	1	0	1	0	3	0	1	0	1	2	84
Ovary	Carcinoma	25	20	171	12	3	150	4	4	17	0	0	3	0	1	0	0	0	0	410
Pancreas	Ductal carcinoma	57	79	1312	312	67	812	0	1	13	0	2	0	0	6	0	0	0	0	2,661
	PanIN	0	3	10	1	0	12	0	0	0	0	0	0	0	0	0	0	0	0	26
	Acinar-ductal metaplasia	0	0	6	0	0	7	0	0	0	0	0	0	0	0	0	0	0	0	13
	Adenoma	6	3	44	13	1	16	0	0	1	0	0	1	0	0	0	0	0	0	85
	Autoimmune pancreatitis	0	0	10	0	0	0	0	0	0	0	0	0	0	0	0	0	0	0	10
	Borderline tumor	0	2	11	2	0	6	0	0	1	0	0	0	0	0	0	0	0	0	22
	Chronic pancreatitis	0	6	42	8	5	21	0	0	0	0	0	0	0	0	0	0	0	0	82
	Dysplasia-*in situ* neoplasm	1	0	24	16	4	17	0	0	1	0	0	0	0	3	0	0	0	0	66
	Hyperplasia	0	7	32	18	4	16	0	1	0	0	0	0	0	3	0	0	0	0	81
Prostate	Adenocarcinoma	0	9	13	1	2	35	0	0	15	0	6	0	0	0	2	0	0	1	84
Skin	Carcinoma	0	2	1	0	1	5	0	0	0	0	0	0	0	1	0	1	0	0	11
	Malignant melanoma	0	0	3	2	1	8	0	0	1	0	0	0	0	1	0	3	0	1	20
Small intestine	Adenocarcinoma	4	8	25	0	4	10	0	0	2	0	0	1	0	1	0	0	0	0	55
Stomach	Adenocarcinoma	20	8	63	1	8	22	0	3	20	0	11	1	0	0	1	1	0	2	161
Thyroid	Carcinoma	5	18	35	4	15	8	1	1	22	2	10	0	0	0	1	0	3	4	129
Urinary tract	Bladder carcinoma	4	4	4	2	4	3	0	0	3	1	0	0	1	1	0	0	0	0	27
Upper aerodigestive	Mouth	1	3	3	1	6	0	0	0	0	0	1	0	0	0	0	0	0	1	16
	Total	496	1367	3,390	488	464	2,219	8	103	686	16	39	15	5	56	12	20	8	21	9,413

(Continued on the following page)

Table 2. Isoform-specific point mutation specificity (Cont'd)

NRAS		Codon 12: GGT						Codon 13: GGT						Codon 61: CAA						
		-C-	T–	-A-	C–	A–	-T-	-C-	T–	-A-	-C–	A–	-T-	G-	–C/T	A–	-T-	-C-	-G-	
Primary tissue	Cancer	12A	12C	12D	12R	12S	12V	13A	13C	13D	13R	13S	13V	61E	61H	61K	61L	61P	61R	Total
H/L	Hematopoietic neoplasm	22	32	185	8	56	31	12	14	93	29	3	29	2	28	24	20	6	29	623
	Lymphoid neoplasm	7	11	60	0	17	11	1	4	54	7	1	6	1	21	37	20	11	27	296
Skin	Benign melanocytic nevus	0	2	4	0	0	0	0	0	0	1	1	0	0	0	55	1	0	35	99
	Carcinoma	0	0	5	0	0	0	0	0	1	0	0	1	0	3	0	0	0	0	10
	Malignant melanoma	2	2	28	5	8	2	1	0	14	12	0	16	1	24	273	64	2	301	755
Thyroid	Adenoma-nodule-goiter	0	1	0	0	0	2	0	1	0	0	0	0	1	1	12	1	0	44	63
	Carcinoma	0	7	2	0	0	0	1	1	1	0	0	0	0	5	32	9	0	182	240
Upper aerodigestive	Larynx	0	0	0	0	20	0	0	0	0	0	0	0	0	0	0	0	0	0	20
	Total	31	55	284	13	101	46	15	20	163	49	5	52	5	82	433	115	19	618	2,106

Data representing the total numbers of tumors with each point mutation were collated from COSMIC v52 release. Single-base mutations that generate each amino-acid substitution are indicated. The most frequent mutations for each isoform for each cancer type are highlighted with gray shading.

Abbreviations: H/L, hematopoietic/lymphoid tissues; PanIN, pancreatic intraepithelial neoplasia.

modes of binding to the target guanine (e.g., *N*-acetoxy-2-acetylaminofluorene) recapitulated this pattern. Of note, although genomic DNA retained this K-Ras codon 12 targeting specificity for DNA adducts, PCR products of the primary target sequences did not (17). This mirrors a discrepancy between the observable BPDE adduct sites in human TP53, which occur at common smoking-related mutation hotspots in lung cancer (18), and the BPDE-induced mutation distribution obtained from a p53 yeast functional assay (19). Because a yeast assay uses a short TP53 cDNA construct rather than the entire gene sequence, the tertiary DNA structure surrounding the mutation hotspots will differ from that found in genomic DNA. These observations suggest that the binding potential of a carcinogen to a target nucleotide in both K-Ras and TP53 depends not only on the very local sequence context but also on the distal sequence and higher DNA organization or modification.

The large-scale, surrounding-sequence context may be an important determinant in shaping the pattern of Ras gene mutations. Whereas the amino-acid sequence encoded by each isoform is almost identical across many species, the DNA sequence shows considerable variation. Exon 1 sequence variation between isoforms could lead to the differential formation of secondary structures, such as hairpin loops, during transcription. Such secondary structures are seen at common TP53 mutation hotspots that have been correlated with a number of predicted stem-loop structures, which suggests that hypermutable bases frequently lie within single-stranded DNA in close proximity to stems (20). In acute myeloid leukemia (AML), K-Ras and N-Ras present a similar distribution of G.C→A.T and G.C→T.A mutations at codon 12. However, analysis of the COSMIC database reveals that the observable rate of mutations is almost 6 times greater for N-Ras compared with K-Ras. The expression level of N-Ras was shown to be elevated relative to K-Ras in AML (21). Assuming a similar etiology for these mutations in either isoform, it is possible that secondary structures that form during increased transcription lead to the higher mutation rate observed for N-Ras in AML tumors. Furthermore, the interplay between the target specificity of a particular mutagen and a transcription-associated local secondary structure could explain the high levels of mutations at codon 12 relative to codon 61 in N-Ras, which are rarely seen in other tumors. Surprisingly, a straightforward analysis of secondary structures has not been performed for codons 12, 13, and 61 in any Ras isoform to date.

Differences in DNA sequence between the Ras isoforms may also influence the repair efficiency of carcinogen adducts. Evidence for this comes from Feng and colleagues (16), who found that repair of BPDE adducts at codon 12 of K-Ras was slower (and thus more inefficient) than that observed for H-Ras and N-Ras. In TP53 it was found that BPDE adducts at major mutation hotspot positions are also regions of slow repair relative to other adduct sites (22). Furthermore, a number of these BPDE adduct sites are associated with low DNA curvature, which is sequence dependent (23). Thus, local and more-distal sequence-context differences in Ras isoforms could result in differences in tertiary structure that substantially influence repair efficiencies.

The collective data provide evidence that increased adduct targeting and relatively poor repair render K-Ras codon 12 far more likely to end up mutated, and provide a plausible explanation for the higher K-Ras mutation rates observed in

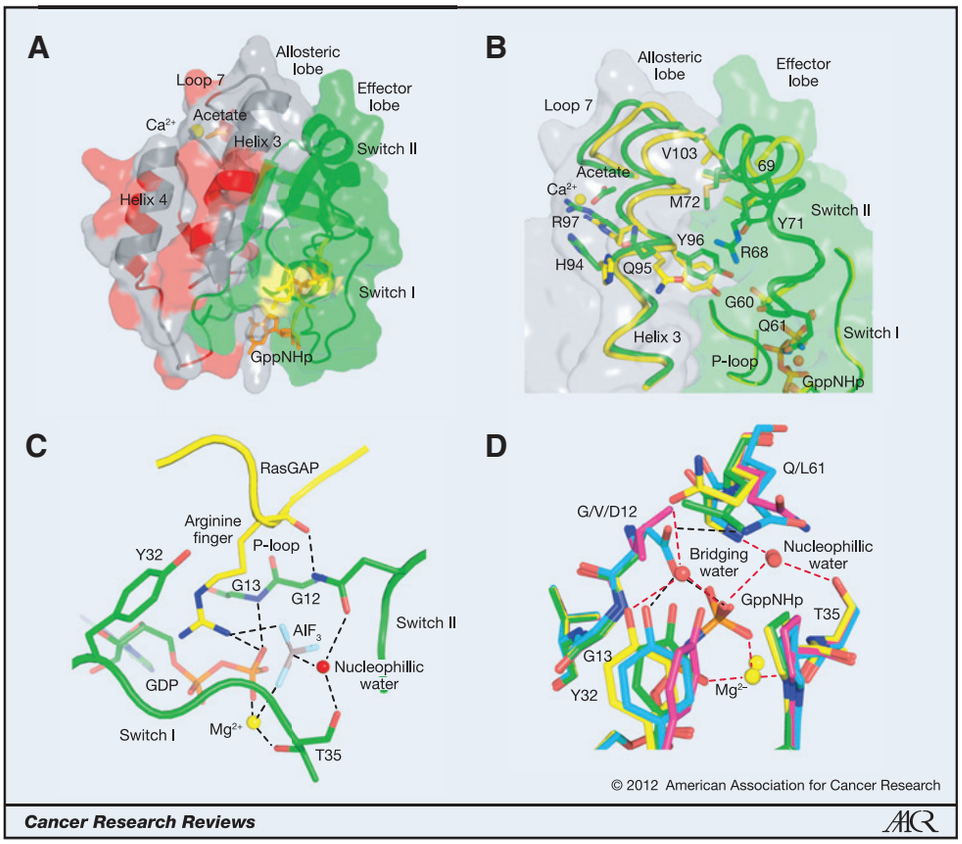

Figure 3. Structural features of Ras and its oncogenic mutations. A, the catalytic domain of Ras. The effector lobe is depicted in green and the allosteric lobe is in gray. Residues that are not identical in all 3 isoforms are in red and are found entirely in the allosteric lobe. Residues 12, 13, and 61 are shown in yellow, and GppNHp is in orange. Calcium acetate is shown bound at the allosteric site. B, the allosteric switch, showing some of the key residues involved. The allosteric state in which switch II is disordered is shown in yellow [Protein Data Bank (PDB) code 2RGE]. Residues 61–68 are disordered and thus were removed from the model. The structure with calcium acetate in the allosteric site that interacts with R97 is shown in green (PDB code 3K8Y). Switch II is ordered in this structure. The nucleotide is depicted in orange. C, the active site in the Ras/RasGAP complex (PDB code 1WQ1). GAP residues are shown in yellow, with the arginine finger shown in stick. Ras residues are in green, including the GDP with phosphate groups in orange. AlF_3 is shown with the aluminum atom in gray and fluorine atoms in cyan. G12, G13, Y32 T35, and Q61 are shown in stick. The Mg^{2+} ion is depicted as a yellow sphere and the nucleophilic water molecule is shown as a red sphere. D, the active site for intrinsic hydrolysis in Ras. The wild type is shown in yellow (PDB code 3K8Y), G12V in magenta (PDB code 3OIW), G12D in cyan (PDB code 1AGP), and Q61L in green (PDB code 3OIU). The wild-type structure contains both nucleophilic and bridging water molecules. Note that in G12D the side chain of D12 replaces the bridging water molecule, whereas in G12V and Q61L there is a direct hydrogen bond between Y32 and the γ-phosphate of the nucleotide. Mg^{2+} is represented by a yellow sphere and water molecules are shown as red spheres in each structure. Hydrogen bonds in the wild-type structure are depicted by red dashed lines, and those in the G12D mutant are indicated by the black dashed line. Hydrogen bonds in the G12V and Q61L structures are not shown. Note the proximity of G13 to the Y32 side chain in the wild-type structure.

cancers. The reasons proposed for these differences in targeting and repair remain speculative. However, it is clear that the 3 Ras genes represent an excellent comparative model system for future investigations of the underlying genetic or epigenetic mechanisms that lead to mutational spectra and hotspots.

Protein-Based Mechanisms

Structural implications of point mutations

The catalytic domain of Ras proteins consists of 2 lobes with an interface that includes switch II on the N-terminal lobe (residues 1–86) and helix 3 on the C-terminal lobe (residues 87–171; Fig. 3A; ref. 24). The first lobe can be thought of as the effector lobe because it contains all of the Ras components that interact with effectors. The second one is the allosteric lobe that interacts with the membrane (25) and exhibits all of the isoform-specific differences outside of the HVR (24). Ras activation in response to the loading of GTP involves large conformational changes in switch I and switch II (26), as well as reorientation with respect to the membrane (27), that promote binding of effector proteins. Given the slow intrinsic hydrolysis rate measured *in vitro* for Ras (28), the deactivation of the signal is critically dependent on enhancement of GTPase activity by GAP (29) or by another mechanism, such as the recently discovered allosteric switch associated with the RAS/RAF/mitogen-activated protein–extracellular signal-regulated kinase (MEK)/extracellular signal-regulated kinase (ERK) pathway (Fig. 3B; refs. 30, 31). In the latter case, a shift in helix

3/loop7 away from switch II is associated with a disorder-to-order transition that brings the catalytic Q61 residue into the active site upon binding of an acidic group, most likely a membrane component, at a remote allosteric site (30). The impaired ability of Ras mutants to hydrolyze GTP, either intrinsically or in response to GAPs, is responsible for the oncogenic nature of mutations at residues G12, G13, and Q61 in the active site. Therefore, it is important to understand the critical roles these residues play in facilitating catalysis.

The structure of Ras in complex with GAP solved in the presence of GDP and AlF_3 mimics the transition state of the hydrolysis reaction, with AlF_3 taking the place of the γ-phosphate in its planar conformation with the nucleophilic water molecule on one side and the GDP leaving group on the other (32). A prominent feature of this structure is the so-called GAP arginine finger that inserts into the RAS active site, providing a positive charge to stabilize the negative charges that accumulate during the course of the hydrolysis reaction (Fig. 3C; ref. 33). The arginine finger is positioned in close van der Waals contact with the Ca atom of G12, leaving no room for any other side chain at this position. Thus, mutants at G12 do not form the transition-state complex with GAPs (34). As exemplified by G12D and G12P (35), as well as by G12V (34), they bind GAP with varying affinities and no increase in hydrolysis rates. Of interest, G12P is the only mutant of G12 that is nontransforming in cells (36), does not appear in any tumors (Table 2), and has a normal or slightly enhanced intrinsic hydrolysis rate (35). Although not much can be found in the literature regarding the structural biology of mutations at G13, it is clear from the Ras/RasGAP structure that any side chain at this position would also clash to some extent with the arginine finger in GAP. Consistently, small side chains at this position, such as G13A and G13V, are able to form the transition-state complex with GAP, but larger ones, such as G13R, cannot (34).

In addition to contributing a catalytic residue, GAP enhances the hydrolysis rate by ordering switch II and placing Q61 in the active site. In doing so, it also promotes a shift in helix 3/loop 7 similar to that described above for the allosteric switch. The amide group of the Q61 side chain hydrogen-bonds to the carbonyl group of the GAP arginine finger, helping to position it in the active site, while its side-chain carbonyl group accepts a hydrogen bond from the nucleophilic water molecule. Glutamine is the only 1 of the 20 amino-acid residues that could serve this dual function, because asparagine would not reach far enough into the active site. Thus, although a mutant such as Q61L can bind GAP with affinity similar to that of the wild type (37), it cannot form the transition-state mimic (34) and its hydrolysis rate is not enhanced by the interaction (38).

The Ras active-site conformation associated with intrinsic hydrolysis is also impaired by the oncogenic mutants at positions 12, 13, and 61 (Fig. 3D; ref. 31). In intrinsic hydrolysis in the presence of Raf, where switch II is proposed to be ordered through the allosteric switch mechanism, the conserved switch I residue Y32 partially overlaps with the position where the GAP arginine finger would bind, and its hydroxyl group is bridged to the γ-phosphate of GTP through a second catalytic water molecule, the bridging water, that also interacts with catalytic residue Q61 (30). Although a structure mimicking the transition state of this reaction is not yet available, it has been proposed that during activation of the nucleophilic water, a proton is shuttled through the γ-phosphate to the bridging water molecule, providing a partial positive charge that stabilizes the negative charges that developed during the reaction in lieu of the GAP arginine finger (30). Mutations at G12 and Q61 exert similar effects by displacing the bridging water molecule and disallowing the positioning of residue 61 as seen in the wild type (Fig. 3D; ref. 31). The structure of G12D shows similar perturbations in the active site, but this time one of its side-chain carboxyl groups takes the place of the bridging water in connecting Y32 to the γ-phosphate of GTP, while its other side-chain oxygen atom hydrogen-bonds to the Q61 side chain (Fig. 3D; ref. 35). All mutants of either G12 (except for G12P) or Q61 result in at least a 10-fold decrease in the intrinsic hydrolysis rate measured *in vitro*. Unfortunately, very little biochemical and structural information about G13 mutants is available, but it is clear that any side chain at this position would clash with the position of Y32 in the active-site conformation associated with intrinsic hydrolysis.

It is clear from the Ras mutational spectra listed in Table 2 that the G12D, G12V, Q61K, Q61L, and Q61R mutations predominate over other mutations. However, although the structural perturbations of the active site caused by these mutants explain how they may contribute to oncogenic transformation, they do not explain their prevalence over other mutants (e.g., G12I and Q61V) that are expected to have similar active-site perturbations and are equally potent in promoting transformation in NIH-3T3 cells (36, 39). *In vitro* experiments indicated that the most highly transforming G12 mutants in cells are I, V, L, T, and R (36). G12I/L/T mutations require more than one base substitution to occur, which explains their relative rarity. In contrast, the highly potent G12R requires only a single substitution of the first base, yet it is also rare. It is notable that the most frequently observed mutations, G12D and G12V, occur after middle-base substitutions. Although there is no obvious protein-structural reason for their predominance, we speculate that their abundance may reflect their relative potency combined with the broad specificity of mutagens for changing the middle base of codon 12.

The situation is much more clear for the Q61 mutants, of which V, L, K, A, C, and R are the most highly transforming mutants in NIH-3T3 cells (39). Of these, only L, K, and R, the predominant Q61 mutants, result from single base changes in the wild-type codon for glutamine. The potency of the highly transforming Q61 mutants derives from the fact that, in addition to perturbing the conformation of the active site, as described above, these mutants shift the conformational equilibrium toward an anticatalytic conformation of switch II when in complex with RAF (40).

Because the effector lobe is identical in all of the isoforms, the isoform-specific preferences for G12, G13, or Q61 mutations shown in Fig. 2 must be due to components that interact with the membrane and are found entirely in the allosteric lobe (Fig. 3A) and the C-terminal HVR. The HVR in particular carries low homology between the isoforms and directs localization in

membrane environments with a distinct composition for each isoform (3). Interaction at the recently discovered allosteric site may be sensitive to the membrane composition, and this site is directly linked to the active site through the allosteric switch, which in turn may be affected differently by the various oncogenic mutations.

Isoform-specific Ras signaling

Distinctive signal outputs by Ras isoforms may also contribute to the bias in Ras mutation frequencies. Although these outputs are almost identical, they are not functionally redundant. The main model currently used to explain isoform-specific Ras signaling involves compartmentalization (3, 41, 42). This model is based on the fact that the only area of significant protein-sequence divergence between the isoforms is in the final 25/26 amino-acid HVR that contains all of the membrane binding and trafficking information (Fig. 1). Although the plasma membrane is the major location for all Ras isoforms, they have also been localized to intracellular membranes such as the endoplasmic reticulum, Golgi, endosomal network, and mitochondria (2). Each isoform is present in these locations in different concentrations due to differences in total abundance, specific targeting, and relative affinity (43–49). These differences in relative localization are believed to enable the Ras isoforms to come into contact with different pools of regulators and effectors to generate overlapping but distinctive outputs.

Investigators have identified more than 20 effectors that can be broadly categorized as kinases or regulators of other GTPases (2). The most important of these are the proliferation-inducing Raf/MEK/ERK kinase cascade and the phosphatidylinositol 3-kinase (PI3K)/protein kinase B (PKB)/Akt pathway that promotes cell survival. *In vitro* experiments have shown that H-Ras is a better activator of PI3K, and K-Ras is more strongly coupled to Raf and Rac (50–52). Of more importance, endogenous isoform-specific differences have been identified in human and mouse development. In humans, germline mutations of each isoform generate overlapping but distinctive sets of neuro-cardio-facial proliferative disorders (53). These mutations also favor Ras activation but are largely distinct from the main oncogenic mutations (Fig. 1). In mice, K-Ras knockout is lethal, whereas N-Ras and H-Ras double-knockout mice apparently develop normally (54–56). Of note, H-Ras is able to substitute for K-Ras when placed under the same endogenous locus (57). Together, these findings indicate that precisely coordinated expression is critical, and argue against the notion that pathways are uniquely regulated by individual isoforms.

Although all 3 of these isoforms have been investigated in terms of their oncogenic signaling properties, relatively few studies have directly compared them. A good *in vitro* model for future work would be the isogenic-cell approach, in which mutant endogenous genes are compared in an identical genetic background. Using this type of approach, Keller and colleagues (58) showed that K-Ras is more potent at generating colorectal cell transformation and modulating signaling than the other isoforms. Equivalent mouse models with oncogenic mutations to endogenous genes have also been instructive. In genetically engineered mice, G12D-mutated K-Ras (but not N-Ras) promoted widespread colonic epithelial hyperplasia as well as neoplasia when combined with the adenomatous polyposis coli mutations commonly seen in colon cancer (59). It was proposed that the unique capacity of K-Ras to promote colorectal adenocarcinoma is linked to proliferative-pathway signaling via Raf, whereas N-Ras triggers cell-survival pathways to inhibit apoptosis (59, 60). Of interest, mutant N-Ras (but not K-Ras) conferred resistance to apoptosis in response to the inflammatory cytokine tumor necrosis factor α, suggesting a model in which the relatively infrequent N-Ras mutations associated with colorectal cancer may be associated with selective pressure exerted by chronic inflammation (60, 61).

The data on isoform-specific signaling are not yet comprehensive; however, it seems clear that the differences are relatively subtle and tissue context specific. This is exemplified by comparative studies that revealed that G12V-mutated K-Ras promotes endodermal stem cell expansion by promoting proliferation and inhibiting differentiation (62). In contrast, mutant N-Ras had no detectable effect, and H-Ras G12V actively promoted differentiation. All of the Ras isoforms differentially used the same effector pathways to achieve these disparate effects (62). These results are significant because many cancers, including pancreatic, lung, and colorectal cancers, are of endodermal origin. These data suggest a model in which K-Ras is coupled to these major types of cancer via its role in expanding cancer progenitor cells in endodermal tissues (1, 63).

It is important to note that signaling is also highly context dependent. The beneficial effects of G13D versus G12D mutations as prognostic indicators for anti-EGFR therapy in advanced colorectal cancer are not evident in non–small cell lung cancer (14, 64). A parallel observation is that the Ras effectors BRAF and PIK3CA are far more frequently mutated in colorectal cancer (11%–13%) than in non–small cell lung cancer (1%–2%) and pancreatic carcinoma (<1%). This implies a different dependency on the activation of specific effector pathways in cancer types that exhibit high rates of KRAS mutations (17%–61%), and suggests differential coupling between KRAS and key effector pathways. In light of the G12D/G13D observations in advanced colorectal cancer, it is also tempting to speculate that specific cancers may be promoted predominantly by upregulation of particular signaling pathways that may be most sensitive to mutations at a given residue. Strong support for this notion comes from work on the Ras allosteric switch that is associated specifically with the Ras/RAF/MEK/ERK pathway, where the Ras–RAF interaction severely impairs hydrolysis in highly transforming Q61 mutants such as Q61L and Q61K (40). Thus, the Q61 mutants are expected to have a very strong oncogenic effect where the RAF pathway is primarily involved in promoting cancer through a malfunction of the allosteric switch. Of interest, N-Ras, for which Q61 mutants are particularly prominent in cancers, is also the only isoform for which a mutation in the allosteric site has been found in tumors (at the R97 position; Fig. 1).

In summary, these data reveal that Ras isoforms are differentially capable of influencing important phenotypic responses that contribute to cancer initiation and progression. K-Ras appears to be the most capable of sustaining cancer programs, and this would translate into strong selective pressure for mutations of this isoform. However, it is striking that despite a prolonged period of investigation, the differences in the signal network responses that are responsible for the preeminence of K-Ras over the other isoforms and their context-dependent signaling remain largely uncharacterized.

Conclusions

We have examined the mutational spectra of 3 Ras isoforms and identified differences that are likely a consequence of multiple interacting intrinsic and extrinsic factors. A tissue-specific comparison among these isoforms indicates that these differences are not simply due to differences in mutagen exposure that could create the heterogeneity observed across a single isoform. We have identified genetic, epigenetic, and protein-based mechanisms that may contribute to generating these mutational spectra. The expression of 3 almost identical Ras isoforms from separate gene loci presents a unique opportunity to deconvolve these mutations. Consequently, this represents an ideal model system for probing generic questions about mutagenesis, carcinogenesis, signaling network integration, and how contextual influences such as relative abundance, tissue expression, and subcellular localization modulate these complex phenomena. We anticipate important advances in our understanding of these areas in the near future with the development of large-scale screening platforms, isogenic model systems, and a more systematic approach toward analyzing the isoforms in parallel.

Disclosure of Potential Conflicts of Interest

No potential conflicts of interest were disclosed.

Acknowledgments

We thank Greg Buhrman for creating Fig. 3.

Grant Support

National Institutes of Health (R56-CA096867); Wellcome Trust, North West Cancer Research Fund, and Biotechnology and Biological Sciences Research Council (I.A. Prior); National Institute for Social Care and Health Research, and Welsh Government (P.D. Lewis).

Received September 12, 2011; revised December 19, 2011; accepted January 13, 2012; published May 16, 2012.

References

1. Quinlan MP, Settleman J. Isoform-specific ras functions in development and cancer. Future Oncol 2009;5:105–16.
2. Omerovic J, Laude AJ, Prior IA. Ras proteins: paradigms for compartmentalised and isoform-specific signalling. Cell Mol Life Sci 2007;64:2575–89.
3. Henis YI, Hancock JF, Prior IA. Ras acylation, compartmentalization and signaling nanoclusters (Review). Mol Membr Biol 2009;26:80–92.
4. Bos JL. ras oncogenes in human cancer: a review. Cancer Res 1989;49:4682–9.
5. Forbes SA, Bindal N, Bamford S, Cole C, Kok CY, Beare D, et al. COSMIC: mining complete cancer genomes in the Catalogue of Somatic Mutations in Cancer. Nucleic Acids Res 2011;39[Database issue]:D945–50.
6. Zarbl H, Sukumar S, Arthur AV, Martin-Zanca D, Barbacid M. Direct mutagenesis of Ha-ras-1 oncogenes by N-nitroso-N-methylurea during initiation of mammary carcinogenesis in rats. Nature 1985;315:382–5.
7. Barbacid M. ras oncogenes: their role in neoplasia. Eur J Clin Invest 1990;20:225–35.
8. Törmänen VT, Pfeifer GP. Mapping of UV photoproducts within ras proto-oncogenes in UV-irradiated cells: correlation with mutations in human skin cancer. Oncogene 1992;7:1729–36.
9. Seo KY, Jelinsky SA, Loechler EL. Factors that influence the mutagenic patterns of DNA adducts from chemical carcinogens. Mutat Res 2000;463:215–46.
10. Le Calvez F, Mukeria A, Hunt JD, Kelm O, Hung RJ, Tanière P, et al. TP53 and KRAS mutation load and types in lung cancers in relation to tobacco smoke: distinct patterns in never, former, and current smokers. Cancer Res 2005;65:5076–83.
11. Hecht SS. Tobacco carcinogens, their biomarkers and tobacco-induced cancer. Nat Rev Cancer 2003;3:733–44.
12. Porta M, Crous-Bou M, Wark PA, Vineis P, Real FX, Malats N, et al. Cigarette smoking and K-ras mutations in pancreas, lung and colorectal adenocarcinomas: etiopathogenic similarities, differences and paradoxes. Mutat Res 2009;682:83–93.
13. Capella G, Cronauer-Mitra S, Pienado MA, Perucho M. Frequency and spectrum of mutations at codons 12 and 13 of the c-K-ras gene in human tumors. Environ Health Perspect 1991;93:125–31.
14. De Roock W, Jonker DJ, Di Nicolantonio F, Sartore-Bianchi A, Tu D, Siena S, et al. Association of KRAS p.G13D mutation with outcome in patients with chemotherapy-refractory metastatic colorectal cancer treated with cetuximab. JAMA 2010;304:1812–20.
15. Sipos JA, Mazzaferri EL. Thyroid cancer epidemiology and prognostic variables. Clin Oncol (R Coll Radiol) 2010;22:395–404.
16. Feng Z, Hu W, Chen JX, Pao A, Li H, Rom W, et al. Preferential DNA damage and poor repair determine ras gene mutational hotspot in human cancer. J Natl Cancer Inst 2002;94:1527–36.
17. Hu W, Feng Z, Tang MS. Preferential carcinogen-DNA adduct formation at codons 12 and 14 in the human K-ras gene and their possible mechanisms. Biochemistry 2003;42:10012–23.
18. Denissenko MF, Pao A, Tang M, Pfeifer GP. Preferential formation of benzo[a]pyrene adducts at lung cancer mutational hotspots in P53. Science 1996;274:430–2.
19. Yoon JH, Lee CS, Pfeifer GP. Simulated sunlight and benzo[a]pyrene diol epoxide induced mutagenesis in the human p53 gene evaluated by the yeast functional assay: lack of correspondence to tumor mutation spectra. Carcinogenesis 2003;24:113–9.
20. Wright BE, Reimers JM, Schmidt KH, Reschke DK. Hypermutable bases in the p53 cancer gene are at vulnerable positions in DNA secondary structures. Cancer Res 2002;62:5641–4.
21. Gougopoulou DM, Kiaris H, Ergazaki M, Anagnostopoulos NI, Grigoraki V, Spandidos DA. Mutations and expression of the ras family genes in leukemias. Stem Cells 1996;14:725–9.
22. Denissenko MF, Pao A, Pfeifer GP, Tang M. Slow repair of bulky DNA adducts along the nontranscribed strand of the human p53 gene may explain the strand bias of transversion mutations in cancers. Oncogene 1998;16:1241–7.
23. Lewis PD, Parry JM. In silico p53 mutation hotspots in lung cancer. Carcinogenesis 2004;25:1099–107.
24. Gorfe AA, Grant BJ, McCammon JA. Mapping the nucleotide and isoform-dependent structural and dynamical features of Ras proteins. Structure 2008;16:885–96.
25. Gorfe AA, Hanzal-Bayer M, Abankwa D, Hancock JF, McCammon JA. Structure and dynamics of the full-length lipid-modified H-Ras protein in a 1,2-dimyristoylglycero-3-phosphocholine bilayer. J Med Chem 2007;50:674–84.

26. Vetter IR, Wittinghofer A. The guanine nucleotide-binding switch in three dimensions. Science 2001;294:1299–304.
27. Abankwa D, Gorfe AA, Hancock JF. Mechanisms of Ras membrane organization and signalling: Ras on a rocker. Cell Cycle 2008;7: 2667–73.
28. John J, Schlichting I, Schiltz E, Rösch P, Wittinghofer A. C-terminal truncation of p21H preserves crucial kinetic and structural properties. J Biol Chem 1989;264:13086–92.
29. Ahmadian MR, Wiesmüller L, Lautwein A, Bischoff FR, Wittinghofer A. Structural differences in the minimal catalytic domains of the GTPase-activating proteins p120GAP and neurofibromin. J Biol Chem 1996;271:16409–15.
30. Buhrman G, Holzapfel G, Fetics S, Mattos C. Allosteric modulation of Ras positions Q61 for a direct role in catalysis. Proc Natl Acad Sci U S A 2010;107:4931–6.
31. Buhrman G, Kumar VS, Cirit M, Haugh JM, Mattos C. Allosteric modulation of Ras-GTP is linked to signal transduction through RAF kinase. J Biol Chem 2011;286:3323–31.
32. Scheffzek K, Ahmadian MR, Kabsch W, Wiesmüller L, Lautwein A, Schmitz F, et al. The Ras-RasGAP complex: structural basis for GTPase activation and its loss in oncogenic Ras mutants. Science 1997;277:333–8.
33. Maegley KA, Admiraal SJ, Herschlag D. Ras-catalyzed hydrolysis of GTP: a new perspective from model studies. Proc Natl Acad Sci U S A 1996;93:8160–6.
34. Gremer L, Gilsbach B, Ahmadian MR, Wittinghofer A. Fluoride complexes of oncogenic Ras mutants to study the Ras-RasGap interaction. Biol Chem 2008;389:1163–71.
35. Franken SM, Scheidig AJ, Krengel U, Rensland H, Lautwein A, Geyer M, et al. Three-dimensional structures and properties of a transforming and a nontransforming glycine-12 mutant of p21H-ras. Biochemistry 1993;32:8411–20.
36. Seeburg PH, Colby WW, Capon DJ, Goeddel DV, Levinson AD. Biological properties of human c-Ha-ras1 genes mutated at codon 12. Nature 1984;312:71–5.
37. Vogel US, Dixon RA, Schaber MD, Diehl RE, Marshall MS, Scolnick EM, et al. Cloning of bovine GAP and its interaction with oncogenic ras p21. Nature 1988;335:90–3.
38. Gibbs JB, Schaber MD, Allard WJ, Sigal IS, Scolnick EM. Purification of ras GTPase activating protein from bovine brain. Proc Natl Acad Sci U S A 1988;85:5026–30.
39. Der CJ, Finkel T, Cooper GM. Biological and biochemical properties of human rasH genes mutated at codon 61. Cell 1986;44:167–76.
40. Buhrman G, Wink G, Mattos C. Transformation efficiency of RasQ61 mutants linked to structural features of the switch regions in the presence of Raf. Structure 2007;15:1618–29.
41. Mor A, Philips MR. Compartmentalized Ras/MAPK signaling. Annu Rev Immunol 2006;24:771–800.
42. Rocks O, Peyker A, Bastiaens PI. Spatio-temporal segregation of Ras signals: one ship, three anchors, many harbors. Curr Opin Cell Biol 2006;18:351–7.
43. Apolloni A, Prior IA, Lindsay M, Parton RG, Hancock JF. H-ras but not K-ras traffics to the plasma membrane through the exocytic pathway. Mol Cell Biol 2000;20:2475–87.
44. Bivona TG, Quatela SE, Bodemann BO, Ahearn IM, Soskis MJ, Mor A, et al. PKC regulates a farnesyl-electrostatic switch on K-Ras that promotes its association with Bcl-XL on mitochondria and induces apoptosis. Mol Cell 2006;21:481–93.
45. Choy E, Chiu VK, Silletti J, Feoktistov M, Morimoto T, Michaelson D, et al. Endomembrane trafficking of ras: the CAAX motif targets proteins to the ER and Golgi. Cell 1999;98:69–80.
46. Rocks O, Gerauer M, Vartak N, Koch S, Huang ZP, Pechlivanis M, et al. The palmitoylation machinery is a spatially organizing system for peripheral membrane proteins. Cell 2010;141:458–71.
47. Roy S, Wyse B, Hancock JF. H-Ras signaling and K-Ras signaling are differentially dependent on endocytosis. Mol Cell Biol 2002;22: 5128–40.
48. Jura N, Scotto-Lavino E, Sobczyk A, Bar-Sagi D. Differential modification of Ras proteins by ubiquitination. Mol Cell 2006;21:679–87.
49. Prior IA, Muncke C, Parton RG, Hancock JF. Direct visualization of Ras proteins in spatially distinct cell surface microdomains. J Cell Biol 2003;160:165–70.
50. Walsh AB, Bar-Sagi D. Differential activation of the Rac pathway by Ha-Ras and K-Ras. J Biol Chem 2001;276:15609–15.
51. Yan J, Roy S, Apolloni A, Lane A, Hancock JF. Ras isoforms vary in their ability to activate Raf-1 and phosphoinositide 3-kinase. J Biol Chem 1998;273:24052–6.
52. Voice JK, Klemke RL, Le A, Jackson JH. Four human ras homologs differ in their abilities to activate Raf-1, induce transformation, and stimulate cell motility. J Biol Chem 1999;274:17164–70.
53. Tidyman WE, Rauen KA. The RASopathies: developmental syndromes of Ras/MAPK pathway dysregulation. Curr Opin Genet Dev 2009;19: 230–6.
54. Esteban LM, Vicario-Abejón C, Fernández-Salguero P, Fernández-Medarde A, Swaminathan N, Yienger K, et al. Targeted genomic disruption of H-ras and N-ras, individually or in combination, reveals the dispensability of both loci for mouse growth and development. Mol Cell Biol 2001;21:1444–52.
55. Koera K, Nakamura K, Nakao K, Miyoshi J, Toyoshima K, Hatta T, et al. K-ras is essential for the development of the mouse embryo. Oncogene 1997;15:1151–9.
56. Umanoff H, Edelmann W, Pellicer A, Kucherlapati R. The murine N-ras gene is not essential for growth and development. Proc Natl Acad Sci U S A 1995;92:1709–13.
57. Potenza N, Vecchione C, Notte A, De Rienzo A, Rosica A, Bauer L, et al. Replacement of K-Ras with H-Ras supports normal embryonic development despite inducing cardiovascular pathology in adult mice. EMBO Rep 2005;6:432–7.
58. Keller JW, Franklin JL, Graves-Deal R, Friedman DB, Whitwell CW, Coffey RJ. Oncogenic KRAS provides a uniquely powerful and variable oncogenic contribution among RAS family members in the colonic epithelium. J Cell Physiol 2007;210:740–9.
59. Haigis KM, Kendall KR, Wang Y, Cheung A, Haigis MC, Glickman JN, et al. Differential effects of oncogenic K-Ras and N-Ras on proliferation, differentiation and tumor progression in the colon. Nat Genet 2008;40:600–8.
60. Kreeger PK, Wang Y, Haigis KM, Lauffenburger DA. Integration of multiple signaling pathway activities resolves K-RAS/N-RAS mutation paradox in colon epithelial cell response to inflammatory cytokine stimulation. Integr Biol (Camb) 2010;2:202–8.
61. Burmer GC, Levine DS, Kulander BG, Haggitt RC, Rubin CE, Rabinovitch PS. c-Ki-ras mutations in chronic ulcerative colitis and sporadic colon carcinoma. Gastroenterology 1990;99:416–20.
62. Quinlan MP, Quatela SE, Philips MR, Settleman J. Activated Kras, but not Hras or Nras, may initiate tumors of endodermal origin via stem cell expansion. Mol Cell Biol 2008;28:2659–74.
63. Quinlan MP, Settleman J. Explaining the preponderance of Kras mutations in human cancer: An isoform-specific function in stem cell expansion. Cell Cycle 2008;7:1332–5.
64. O'Byrne KJ, Gatzemeier U, Bondarenko I, Barrios C, Eschbach C, Martens UM, et al. Molecular biomarkers in non-small-cell lung cancer: a retrospective analysis of data from the phase 3 FLEX study. Lancet Oncol 2011;12:795–805.
65. Cox AD, Der CJ. Ras history: the saga continues. Small Gtpases 2010;1:2–27.
66. Goody RS, Pai EF, Schlichting I, Rensland H, Scheidig A, Franken S, et al. Studies on the structure and mechanism of H-ras p21. Philos Trans R Soc Lond B Biol Sci 1992;336:3–10; discussion 10-1.